X-Ray Crystal Structures and Magnetic Properties of Azide-bridged Binuclear Copper(II) Complexes containing the Schiff-base Ligand derived from 2-Pyridinecarbaldehyde and Histamine. Structure–Magnetism Relationship†

Keiji Matsumoto,* Shun'ichiro Ooi, and Kunio Nakatsuka
Department of Chemistry, Faculty of Science, Osaka City University, Sumiyoshi-ku, Osaka 558, Japan
Wasuke Mori, Shinnichiro Suzuki, and Akitsugu Nakahara
Institute of Chemistry, College of General Education, Osaka University, Toyonaka, Osaka 560, Japan
Yasuo Nakao
Chemical Laboratory, Faculty of Education, Okayama University, Okayama 700, Japan

The structures of the complexes $[Cu_2(L^1)_2(N_3)_2][ClO_4]_2$ (**1**) {L^1 = 1-(imidazol-4-yl)-2-[(2-pyridylmethylene)amino]ethane} and $[Cu_2(L^1)_2(N_3)_3]Cl{\cdot}2H_2O$ (**2**) have been determined by *X*-ray methods. Complex (**1**) contains discrete $[Cu_2(L^1)_2(N_3)_2]^{2+}$ cations which are located at centres of inversion. The geometry around each copper(II) ion is square pyramidal. The two basal planes in the complex cation are parallel and separated by 2.64 Å. The two azide ions which are parallel to each other bridge in an end-on fashion between a basal position of one square pyramid and an apical position of the other. Magnetic susceptibility data for (**1**) show a ferromagnetic interaction (Weiss constant θ = +23 K) above 200 K. On the other hand, below 200 K, it is considered that there is a weaker exchange interaction than that above 200 K. In differential scanning calorimetry curves for (**1**), small thermal anomalies have been observed over the temperature range 150—250 K. Complex (**2**) contains an azide-bridged, centrosymmetric copper(II) dimeric cation. The five-co-ordinate geometry around each copper(II) ion is square pyramidal. An azide ion bridges in an end-to-end fashion between the two apical positions of two square pyramids. A very weak antiferromagnetic exchange interaction is found for (**2**) ($0 \geqslant J \geqslant -0.5$ cm^{-1}, where J denotes the exchange integral defined by the Hamiltonian $\mathscr{H} = -2JS_1S_2$).

Binuclear copper(II) complexes bridged by an azide ion have been studied by many investigators with a view to understanding the relationship between their structures and magnetic properties.[1–14] The diamagnetic complexes among these compounds are of interest as models for the active site of Type III copper-containing proteins, in which a pair of copper(II) ions are strongly coupled antiferromagnetically. In connection with these investigations, we have recently described the preparation and magnetic properties of a number of azide-bridged copper(II) Schiff-base complexes.[15] Since we have obtained single crystals of $[Cu_2(L^1)_2(N_3)_2][ClO_4]_2$ (**1**) and $[Cu_2(L^1)_2(N_3)_3]Cl{\cdot}2H_2O$ (**2**) containing the Schiff-base ligand L^1, their *X*-ray structure analyses have been carried out in order to study the structure–magnetism relationship. Measurements of variable-temperature magnetic susceptibility and differential scanning calorimetry (d.s.c.) were performed for (**1**) and also for $[Cu_2(L^2)_2(N_3)_2]{\cdot}2H_2O$ (**3**) {HL^2 = 3-[(2-pyridylmethylene)amino]propionic acid} and the results discussed.

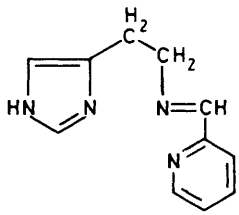

L^1

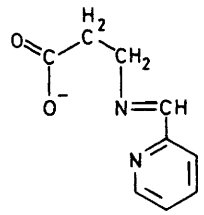

L^2

Experimental

X-Ray Data Collection.—Preparations of (**1**) and (**2**) were described previously.[15] Crystals of (**1**) and (**2**) were mounted in an arbitrary orientation on a Philips PW1100 automated diffractometer. The PW1100 programs obtained 18 centred reflections for (**1**) and 17 for (**2**), an orientation matrix for each crystal, and then identified the monoclinic cell for (**1**) and the triclinic cell for (**2**). The space group $P\bar{1}$ for (**2**) was assumed throughout the structure analysis and was confirmed by the successful refinement of the structure. The unit-cell dimensions were refined by least-squares analyses of the θ values of 19 reflections for (**1**) and 13 for (**2**). The crystal data and experimental details are given in Table 1. Intensity data were collected by the use of Mo-K_α radiation (λ = 0.7107 Å). During the data collection, three standard reflections were monitored every 3 h to check the stability and orientation of each crystal. No appreciable decay was observed. Each data set was corrected for Lorenz–polarization effects,[16] but not for absorption.

Structure Solution and Refinement.—The structure of (**1**) was solved by conventional Patterson–Fourier methods, while that of (**2**) was solved by the use of MULTAN.[17] Refinement of the structures was carried out by block-diagonal least squares. The function minimized was $\Sigma w(F_o - |F_c|)^2$, where $w = 1/\sigma^2(F_o)$. Atomic scattering factors for the Cu, Cl, Cl^-, O, N, C, and H atoms were taken from ref. 18, with anomalous dispersion corrections ($\Delta f'$) for the Cu, Cl, and Cl^- atoms. The final R values were 0.043 for (**1**) and 0.042 for (**2**). The hydrogen atoms defined by the geometry of the complexes were located at calculated positions (N–H, C–H = 1.0 Å). The hydrogen atoms of the water molecules in (**2**) could not be found in the difference

† *Supplementary data available* (No. SUP 56268, 15 pp.): H-atom co-ordinates, full bond distances and angles, thermal parameters. See Instructions for Authors, *J. Chem. Soc., Dalton Trans.*, 1985, Issue 1, pp. xvii—xix. Structure factors are available from the editorial office.

Non-S.I. units employed: G = 10^{-4} T, $\chi_{c.g.s.u.} = \chi_{S.I.} \times 10^6/4\pi$.

Table 1. Crystal data for complexes $[Cu_2(L^1)_2(N_3)_2][ClO_4]_2$ (**1**) and $[Cu_2(L^1)_2(N_3)_3]Cl{\cdot}2H_2O$ (**2**)

Complex	(1)	(2)
Formula	$C_{22}H_{24}Cl_2Cu_2N_{14}O_8$	$C_{22}H_{28}ClCu_2N_{17}O_2$
M	810.6	725.2
Crystal system	Monoclinic	Triclinic
Space group	$P2_1/c$	$P\bar{1}$
a/Å	9.654(4)	21.770(9)
b/Å	11.158(3)	9.910(3)
c/Å	14.625(6)	7.582(3)
α/°		112.50(3)
β/°	106.49(2)	90.03(3)
γ/°		98.02(3)
U/Å^3	1 510.7(10)	1 494.0(9)
F(000)	820	740
Z	2	2
D_m/g cm^{-3}	1.77	1.28
D_c/g cm^{-3}	1.78	1.30
μ(Mo-K_α)/cm^{-1}	17.1	16.2
Crystal dimensions/mm	0.24 × 0.29 × 0.30	0.08 × 0.18 × 0.42
Scan type	ω	ω
Scan speed/° s^{-1}	0.033	0.033
Scan range/°	1.0 + 0.2 tanθ	1.0
2θ max/°	50	50
Background measurement/s	half of the scan time on each side of the scan range	15
Number of reflections	2 036 [$\geqslant 2\sigma(F_o^2)$]	3 259 [$\geqslant 3\sigma(F_o^2)$]
R	0.043	0.042
$R' = (\Sigma w\Delta F^2/\Sigma wF_o^2)^{\frac{1}{2}}$	0.052	0.049

Table 2. Atomic co-ordinates for $[Cu_2(L^1)_2(N_3)_2][ClO_4]_2$ (**1**) with estimated standard deviations in parentheses

Atom	x	y	z
Cu	0.180 70(6)	0.024 91(5)	0.534 86(4)
Cl	0.405 43(15)	0.464 15(12)	0.300 13(9)
N(1)	0.366 4(5)	−0.293 8(4)	0.490 9(3)
N(2)	0.265 1(4)	−0.120 3(4)	0.495 9(3)
N(3)	0.277 7(4)	0.127 6(4)	0.456 4(3)
N(4)	0.140 2(4)	0.189 5(3)	0.581 4(3)
N(5)	0.050 3(4)	−0.053 6(3)	0.599 0(3)
N(6)	0.063 2(4)	−0.154 5(4)	0.627 7(3)
N(7)	0.068 9(5)	−0.252 3(4)	0.655 6(3)
C(1)	0.309 5(5)	−0.222 0(4)	0.543 1(4)
C(2)	0.358 9(6)	−0.238 0(5)	0.406 0(4)
C(3)	0.296 6(5)	−0.130 6(5)	0.408 7(4)
C(4)	0.270 8(6)	−0.030 2(5)	0.339 4(4)
C(5)	0.343 9(6)	0.083 5(5)	0.384 5(4)
C(6)	0.262 3(6)	0.239 0(5)	0.466 5(4)
C(7)	0.189 1(6)	0.278 7(4)	0.536 1(4)
C(8)	0.164 3(6)	0.398 5(5)	0.551 4(4)
C(9)	0.083 6(7)	0.426 1(5)	0.612 7(4)
C(10)	0.032 9(7)	0.335 7(5)	0.656 6(4)
C(11)	0.064 1(6)	0.218 3(5)	0.640 6(4)
O(1)	0.267 5(5)	0.465 2(5)	0.318 7(4)
O(2)	0.507 6(6)	0.500 4(4)	0.385 7(4)
O(3)	0.437 5(6)	0.347 4(4)	0.276 5(4)
O(4)	0.400 4(5)	0.545 1(5)	0.226 0(4)

synthesis. No chemically significant peaks were observed on the final difference-Fourier maps. Maximum peaks were 0.5 e Å^{-3} for (**1**) and (**2**). In the final cycles of refinement the hydrogen atoms were included with a common isotropic thermal parameter, B = 4.0 Å^2, but their parameters were not refined.

The atomic co-ordinates are given in Tables 2 and 3. Figures 1 and 2 were drawn by the use of ORTEP.[19] Computations were performed using the programs in the UNICS[20] on the FACOM 230-60 computer at Osaka City University and the ACOS-850 computer at the Crystallographic Research Centre, Institute for Protein Research, Osaka University.

Table 3. Atomic co-ordinates for $[Cu_2(L^1)_2(N_3)_3]Cl{\cdot}2H_2O$ (**2**) with estimated standard deviations in parentheses

Atom	x	y	z
Cu(A)	0.021 06(3)	0.698 45(8)	0.088 56(9)
N(A1)	−0.145 3(2)	0.819 1(6)	0.299 7(7)
N(A2)	−0.055 4(2)	0.744 7(5)	0.222 0(6)
N(A3)	0.073 2(2)	0.784 3(5)	0.339 5(6)
N(A4)	0.106 3(2)	0.665 9(5)	−0.011 6(6)
N(A5)	−0.019 6(2)	0.559 6(5)	−0.159 6(6)
N(A6)	−0.070 9(2)	0.553 1(5)	−0.226 1(6)
N(A7)	−0.119 3(3)	0.540 2(6)	−0.298 6(7)
N(A8)	0.0	1.000 0	0.0
N(A9)	0.035 2(3)	0.926 7(6)	0.025 3(7)
C(A1)	−0.105 7(3)	0.778 0(7)	0.160 5(8)
C(A2)	−0.118 6(3)	0.813 3(7)	0.462 5(8)
C(A3)	−0.062 7(3)	0.766 3(6)	0.411 7(8)
C(A4)	−0.013 3(3)	0.748 1(6)	0.534 9(8)
C(A5)	0.048 5(3)	0.839 7(6)	0.533 2(8)
C(A6)	0.130 0(3)	0.775 4(7)	0.321 1(8)
C(A7)	0.151 8(3)	0.713 8(7)	0.127 6(8)
C(A8)	0.213 5(3)	0.704 5(8)	0.087 9(10)
C(A9)	0.228 4(3)	0.643 9(9)	−0.100 2(10)
C(A10)	0.182 3(3)	0.595 4(8)	−0.241 4(9)
C(A11)	0.121 2(3)	0.607 7(7)	−0.193 8(8)
Cu(B)	0.478 95(3)	0.301 66(8)	0.390 33(9)
N(B1)	0.645 1(3)	0.181 1(6)	0.481 4(7)
N(B2)	0.555 5(2)	0.255 2(5)	0.477 3(6)
N(B3)	0.427 0(2)	0.216 5(5)	0.555 6(6)
N(B4)	0.393 8(2)	0.333 6(5)	0.322 8(6)
N(B5)	0.519 7(2)	0.441 5(5)	0.280 7(7)
N(B6)	0.570 6(2)	0.446 9(5)	0.220 3(6)
N(B7)	0.619 3(3)	0.459 2(6)	0.161 2(8)
N(B8)	0.500 0	0.0	0.0
N(B9)	0.464 9(3)	0.072 7(6)	0.098 6(7)
C(B1)	0.605 8(3)	0.222 4(7)	0.382 4(8)
C(B2)	0.618 7(3)	0.187 5(7)	0.649 3(8)
C(B3)	0.562 8(3)	0.232 3(6)	0.645 4(7)
C(B4)	0.513 4(3)	0.252 4(6)	0.785 9(8)
C(B5)	0.451 3(3)	0.160 3(7)	0.692 0(8)
C(B6)	0.369 9(3)	0.224 2(7)	0.546 2(8)
C(B7)	0.348 0(3)	0.286 7(6)	0.413 3(8)
C(B8)	0.286 5(3)	0.297 0(8)	0.385 3(10)
C(B9)	0.271 4(3)	0.356 3(8)	0.256 6(10)
C(B10)	0.317 6(3)	0.404 3(8)	0.162 0(9)
C(B11)	0.378 7(3)	0.392 6(7)	0.199 8(8)
Cl	0.749 99(9)	−0.000 20(22)	0.280 24(24)
O(1)	0.165 6(3)	0.049 9(6)	0.099 2(7)
O(2)	0.665 8(3)	0.050 9(6)	0.951 1(7)

Measurements.—Magnetic susceptibility measurements over the temperature range of liquid helium to room temperature were carried out by the Faraday method. The instrument was calibrated with $CuSO_4{\cdot}5H_2O$. The d.s.c. experiments were carried out by the use of a Rigaku 8001SL differential scanning calorimeter. Powdered X-band e.s.r. spectra at room temperature and 77 K were recorded by the method reported previously.[15]

Results and Discussion

Figure 1 shows a view of the discrete complex cation in (**1**). The complex ion is dimeric and has a crystallographic centre of inversion. The co-ordination geometry about the five-co-ordinate Cu^{II} ion is described as a square pyramid. The

Table 4. Interatomic distances (Å) and angles (°) for (**1**) with estimated standard deviations in parentheses

Cu–N(2)	1.969(4)	N(2)–Cu–N(3)	90.3(2)
Cu–N(3)	2.028(4)	N(3)–Cu–N(4)	81.0(2)
Cu–N(4)	2.034(4)	N(4)–Cu–N(5)	91.9(2)
Cu–N(5)	1.975(4)	N(5)–Cu–N(2)	98.3(2)
N(2)–C(3)	1.397(6)	N(2)–Cu–N(5)*	103.1(3)
C(3)–C(4)	1.483(7)	N(3)–Cu–N(5)*	86.5(3)
C(4)–C(5)	1.510(7)	N(4)–Cu–N(5)*	86.2(3)
N(3)–C(5)	1.463(7)	N(5)–Cu–N(5)*	83.3(3)
N(3)–C(6)	1.266(6)	Cu–N(5)–Cu*	96.7(2)
C(6)–C(7)	1.463(8)	N(6)–N(5)–Cu*	111.8(3)
N(4–C(7)	1.353(6)	Cu–N(5)–N(6)	124.6(3)
N(5)–N(6)	1.196(5)	N(5)–N(6)–N(7)	176.8(5)
N(6)–N(7)	1.161(6)		
Cu–N(5)*	2.536(4)		
Cu···Cu*	3.391(2)		

Short contacts less than 3.1 Å

N(1)···O(2) ($1-x, -y, 1-z$)	2.968(7)
Cu···O(4) ($x, \frac{1}{2}-y, \frac{1}{2}+z$)	3.092(5)

* Atoms at symmetry position $-x, -y, 1-z$.

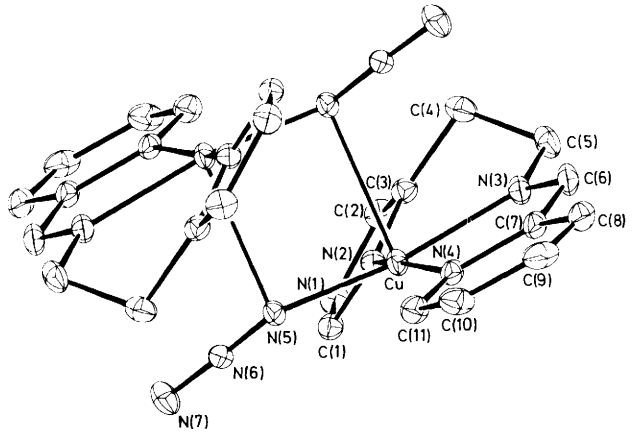

Figure 1. Structure of the complex cation in (**1**)

three nitrogen atoms [N(2), N(3), N(4)] of L^1 and the azide nitrogen atom N(5) comprise the basal plane, whereas the apical position is occupied by the N(5) ($-x, -y, 1-z$) atom of the second azide ligand. A least-squares plane calculation for the square plane shows that the four nitrogen atoms tetrahedrally deviate from the plane, deviations of the atoms from the least-squares plane being N(2) −0.149(4), N(3) 0.169(4), N(4) −0.167(4), N(5) 0.147(4), Cu −0.002(2), N(6) −0.198(5), N(7) −0.495(6) Å. The N(5)–N(6) bond inclines to the least-squares plane at 16.8°. The bond lengths in the basal plane range from 1.969(4) to 2.034(4) Å and the apical Cu–N bond length is 2.536(4) Å (Table 4). The co-ordination of the bridging N_3^- anion to the two Cu^{II} ions is unsymmetrical. The N(6)–N(5)–Cu angle of 124.6(3)° is larger than the N(6)–N(5)–Cu ($-x, -y, 1-z$) angle of 111.8(3)° and the Cu–N(5) ($-x, -y, 1-z$) distance [2.536(4) Å] is ~0.6 Å longer than Cu–N(5) [1.975(4) Å]. The [Cu,N(5),Cu ($-x, -y, 1-z$), N(5) ($-x, -y, 1-z$)] plane and the N(5)–N(6) bond make an angle of 44.4°. The Cu···Cu distance in the dimeric cation is 3.391(2) Å. The O(4) atom ($x, \frac{1}{2}-y, \frac{1}{2}-z$) from ClO_4^- approaches the Cu atom at 3.092(5) Å from the other side of the square pyramid. For L^1 the [Cu,N(2),N(3), C(3),C(4),C(5)] six-membered ring constitutes a boat conformation. The other six- and five-membered rings are approximately planar (maximum deviation 0.03 Å).

Table 5. Interatomic distances (Å) and angles (°) for (**2**) with estimated standard deviations in parentheses

Cu(A)–N(A2)	1.965(4)	N(A2)–Cu(A)–N(A3)	91.6(2)
Cu(A)–N(A3)	2.030(4)	N(A3)–Cu(A)–N(A4)	80.2(2)
Cu(A)–N(A4)	2.026(4)	N(A4)–Cu(A)–N(A5)	91.2(2)
Cu(A)–N(A5)	1.974(4)	N(A5)–Cu(A)–N(A2)	96.8(2)
Cu(A)–N(A9)	2.465(6)	N(A2)–Cu(A)–N(A9)	92.9(2)
N(A8)–N(A9)	1.189(6)	N(A3)–Cu(A)–N(A9)	96.0(2)
Cu(B)–N(B2)	1.967(5)	N(A4)–Cu(A)–N(A9)	87.3(2)
Cu(B)–N(B3)	2.027(5)	N(A5)–Cu(A)–N(A9)	99.1(2)
Cu(B)–N(B4)	2.022(5)	Cu(A)–N(A9)–N(A8)	133.3(3)
Cu(B)–N(B5)	1.984(5)	N(B2)–Cu(B)–N(B3)	91.6(2)
Cu(B)–N(B9)	2.470(4)	N(B3)–Cu(B)–N(B4)	80.1(2)
N(B8)–N(B9)	1.185(5)	N(B4)–Cu(B)–N(B5)	91.3(2)
Cu(A)···Cu(A)	6.785(2)	N(B5)–Cu(B)–N(B2)	96.9(2)
Cu(B)···Cu(B)	6.788(2)	N(B2)–Cu(B)–N(B9)	92.7(2)
		N(B3)–Cu(B)–N(B9)	96.1(2)
		N(B4)–Cu(B)–N(B9)	87.4(2)
		N(B5)–Cu(B)–N(B9)	99.2(2)
		Cu(B)–N(B9)–N(B8)	133.3(3)
		Cu(A)–N(A5)–N(A6)	128.7(3)
		N(A5)–N(A6)–N(A7)	176.1(5)
		Cu(B)–N(B5)–N(B6)	128.3(4)
		N(B5)–N(B6)–N(B7)	176.3(6)

Short contacts

Cl···C(1) ($1-x, -y, -z$)	3.327(5)
Cl···C(2) ($x, y, -1+z$)	3.327(6)
Cl···N(A1) ($1+x, -1+y, z$)	3.125(6)
C(1)···N(A9) ($x, -1+y, z$)	2.894(7)
C(2)···N(B9) ($1-x, -y, 1-z$)	2.899(7)
Cu(A)···N(A5) ($-x, 1-y, -z$)	2.804(6)
Cu(B)···N(B5) ($1-x, 1-y, 1-z$)	2.797(5)
Cu(A)···Cu(A) ($-x, 1-y, -z$)	3.615(2)
Cu(B)···Cu(B) ($1-x, 1-y, 1-z$)	3.612(2)

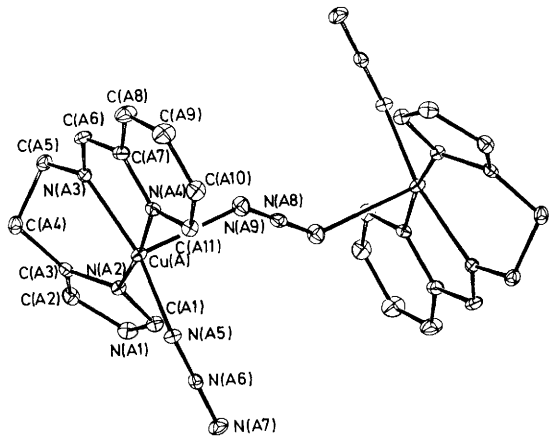

Figure 2. Structure of a complex cation in (**2**); the other crystallographically independent complex cation is similarly labelled by the use of B

Figure 2 shows a perspective view of one of the two dimeric cations in (**2**). The two crystallographically independent cations A and B are essentially identical. The complex cation has end-to-end azide bridging, and is located at a crystallographic centre of inversion. The local environment at each Cu^{II} ion is described as a square pyramid. The apical position is occupied by N(A9) or N(B9) of the bridging azide ion, whereas the basal planes are defined by the N(A2), N(A3), N(A4), and N(A5) atoms of one

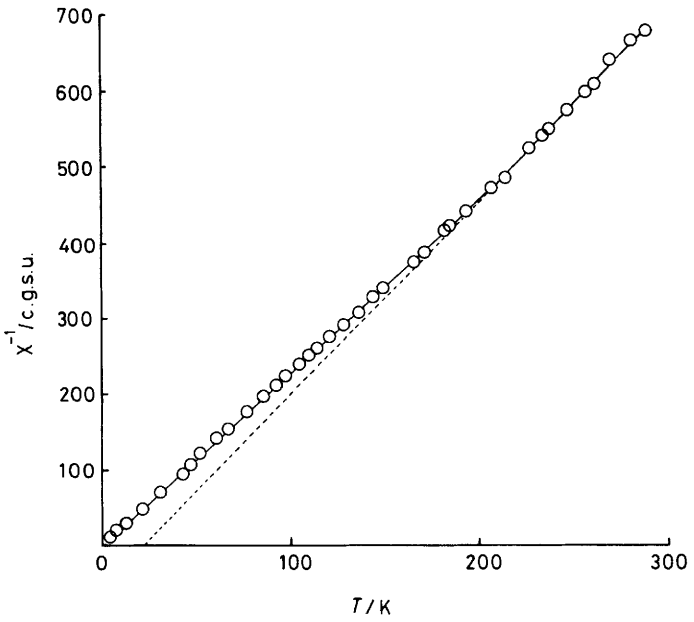

Figure 3. Temperature dependence of the magnetic susceptibility of (**1**). Dotted intercept $\theta = +23$ K

complex ion and by the N(B2), N(B3), N(B4), and N(B5) atoms of the other. The basal planes are tetrahedrally distorted, the deviations of the atoms from each least-squares plane being N(A2) 0.123(6), N(A3) −0.139(6), N(A4) 0.139(6), N(A5) −0.123(6), Cu(A) 0.139(3), N(A6) 0.153(8), N(A7) 0.39(1), N(A9) 2.601(7), N(B2) 0.125(4), N(B3) −0.143(4), N(B4) 0.143(4), N(B5) −0.125(4), Cu(B) 0.140(2), N(B6) 0.158(6), N(B7) 0.396(7), N(B9) 2.606(5) Å. The least-squares plane and the Cu(A)–N(A9) bond make an angle of 87.0° and the angle between the least-squares plane and the linear bridging azide ion is 46.3°. The corresponding angles in the other dimer are 88.6 and 44.6° respectively. The basal Cu–N bonds range from 1.965(4) to 2.030(4) Å (Table 5). The Cu–N apical bond lengths are 2.465(6) and 2.470(4) Å for A and B respectively. The Cu ••• Cu distances in the dimers are 6.785(2) for A and 6.788(2) Å for B. The opposite side of the square pyramid containing Cu(A) is occupied by N(A5) $(-x, 1-y, -z)$ at 2.804(5) Å and that containing Cu(B), by N(B5) $(1-x, 1-y, 1-z)$ at 2.797(5) Å. These Cu–N distances are close to the longest limit of semi-co-ordination.[21] The structure could be regarded as a chain, however, the Cu(A)–N(A9) [Cu(B)–N(B9)] distance is ~0.3 Å shorter than the intermolecular distance Cu(A) ••• N(A5) [Cu(B) ••• N(B5)] and thus the structure is better described as a dimer rather than a chain. The half-field absorption in the $\Delta M_s = 2$ region of the powdered *X*-band e.s.r. spectrum was observed in (**2**).[15]

Structure–Magnetism Relationship.—When an azide ion bridges two copper(II) ions, two types of bridging mode are expected. One is the end-on type, and the other end-to-end. End-on type bridging has been found in (**1**). As is clear from Figure 3, variable-temperature magnetic susceptibility data for (**1**) suggest that the two copper(II) ions are coupled in a ferromagnetic manner (Weiss constant $\theta = +23$ K) above 200 K. As the apical Cu–N distance in the dimer is 2.536(4) Å, it seems that the ferromagnetic spin–spin coupling occurs *via* the Cu–N–Cu bridge. A similar type of ferromagnetic interaction between two copper(II) ions has been found for a variety of binuclear copper(II) complexes.[22] At *ca.* 200 K, the susceptibility–temperature line deviates sharply from the expected χ^{-1} *versus* *T* plot of a ferromagnetically coupled Cu^{II}–Cu^{II} dimer,

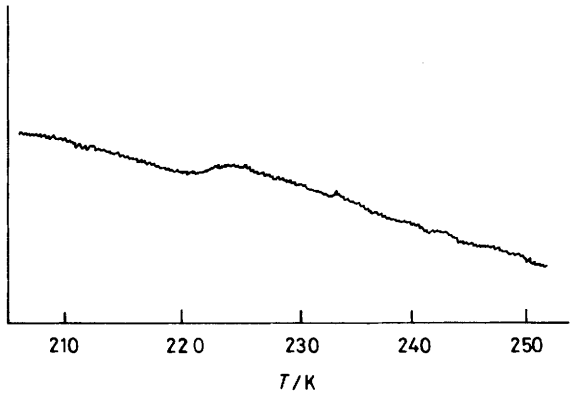

Figure 4. Differential scanning calorimetric curve (arbitrary scale) of (**1**) at a heating rate of 5 K min^{-1}

thus indicating the presence of a phase transition. Below 200 K, the two copper(II) ions are thus apparently non-coupled, due perhaps, to a change in Cu–N–Cu angle and/or Cu–N bond lengths. Differential scanning calorimetry (d.s.c.) curves for (**1**) show small thermal anomalies over the temperature range 150—250 K. From curves taken at various scan rates, the transition rate was found to be appreciably slow. The chart for the sample annealed at 213 K for 60 min indicates the existence of a single broad endotherm at *ca.* 220 K (Figure 4). The transition temperatures obtained by d.s.c. and that by the magnetic method were virtually the same. The enthalpy of transition was determined to be 1.24 kJ mol^{-1}. The transition entropy, 5.6 J K^{-1} mol^{-1}, is approximately equal to $R \ln 2$. Also, the half-field $\Delta M_s = 2$ signal at *ca.* 1 500 G was clearly observed for (**1**) in the powder *X*-band e.s.r. spectrum (77 K). This implies the presence of an exchange interaction between the two copper(II) ions at 77 K. From these results it is considered that there is a weaker exchange interaction below 200 K than above.

Several papers[10,11,13,14] have been published concerning the structure–magnetism relationship for binuclear copper(II) complexes bridged by end-on type azide ions. However, in these

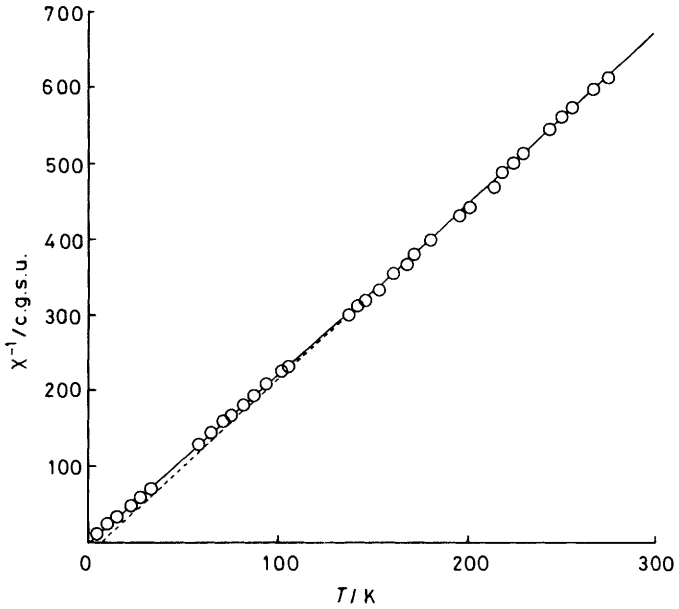

Figure 5. Temperature dependence of the magnetic susceptibility of $[Cu_2(L^2)_2(N_3)_2]\cdot 2H_2O$ (**3**). Dotted intercept $\theta = +7$ K

complexes, the two copper co-ordination planes were nearly coplanar and the azide ion bridged the two copper(II) ions in the co-ordination plane. The coupling between the two copper(II) ions was reported to be ferromagnetic[10,11,13,14] and stronger than the coupling of the present complex. In the structure of (**1**), the two copper co-ordination planes are separated by 2.64 Å and the azide ion bridges between a basal position of one square pyramid and an apical position of the other. The geometrical situation in (**1**) makes it impossible for the two unpaired electrons to exchange extensively through the bridging azide ion, resulting in a weaker ferromagnetic interaction than observed in the previously reported complexes.[10,11,13,14] The present result also lends support to the presence of ferromagnetic coupling when azide ions bridge in an end-on-fashion.[2,10,11,13,14]

We also prepared the complex $[Cu_2(L^2)_2(N_3)_2]\cdot 2H_2O$ (**3**)[15] and its magnetic behaviour is shown in Figure 5. As in the case of (**1**), a weak ferromagnetic interaction (Weiss constant $\theta = +7$ K) was observed above 200 K. The d.s.c. chart of (**3**) gave a small broad endotherm at 199 K. The enthalpy of transition was estimated as 1.32 kJ mol^{-1}. The structure of (**3**) is, therefore, considered to be similar to that of (**1**) with end-on azide bridging.

The magnetic susceptibility data down to 4.2 K for (**2**) showed only a very weak antiferromagnetic exchange interaction ($0 \geqslant J \geqslant -0.5$ cm^{-1}).[15] The azide ion bridges two apical positions of two square pyramids in an end-to-end type mode. The e.s.r. spectrum was indicative of a $d_{x^2-y^2}$ ground state.[15] The co-ordination geometries around the two copper(II) ions in (**2**) were again unfavourable for exchanging two unpaired electrons through the bridging azide ion. The structure and magnetic behaviour of (**2**) are essentially similar to those reported by Drew *et al.*[6] Antiferromagnetic interactions have also been found in many complexes[5,7,9,12] which have end-to-end azide bridging. Generally the end-to-end azide bridging seems to be the direct cause of the antiferromagnetic coupling.

Metazidohemocyanins were prepared by adding excess azide ion to solutions of hemocyanins of *Busycon canaliculatum* and *Limulus polyphemus*.[23,24] It has been pointed out that these metazidohemocyanins contain antiferromagnetically coupled copper(II) ions, the azide ion bridging two copper(II) ions in an end-to-end fashion.[23,24] We support this conclusion from the structure–magnetism relationship mentioned above.

References

1 D. M. Duggan and D. N. Hendrickson, *Inorg. Chem.*, 1973, **12**, 2422.
2 C. G. Barraclough, R. W. Brookes, and R. L. Martin, *Aust. J. Chem.*, 1974, **27**, 1843.
3 G. R. Hall, D. M. Duggan, and D. N. Hendrickson, *Inorg. Chem.*, 1975, **14**, 1956.
4 T. R. Felthouse, E. J. Laskowski, D. S. Bieksza, and D. N. Hendrickson, *J. Chem. Soc., Chem. Commun.*, 1976, 777.
5 T. R. Felthouse and D. N. Hendrickson, *Inorg. Chem.*, 1978, **17**, 444.
6 M. G. B. Drew, M. McCann, and S. M. Nelson, *J. Chem. Soc., Chem. Commun.*, 1979, 481.
7 Y. Agnus, R. Louis, and R. Weiss, *J. Am. Chem. Soc.*, 1979, **101**, 3381.
8 Y. Agnus, R. Louis, J-P. Gisselbrecht, and R. Weiss, *J. Am. Chem. Soc.*, 1984, **106**, 93.
9 V. McKee, J. V. Dagdigian, R. Bau, and C. A. Reed, *J. Am. Chem. Soc.*, 1981, **103**, 7000.
10 J. Comarmond, P. Plumere, J-M. Lehn, Y. Agnus, R. Louis, R. Weiss, O. Kahn, and I. Morgenstern-Badarau, *J. Am. Chem. Soc.*, 1982, **104**, 6330.
11 O. Kahn, *Inorg. Chim. Acta*, 1982, **62**, 3.
12 I. Bkouche-Waksman, S. Sikorav, and O. Kahn, *J. Crystallogr. Spectrosc. Res.*, 1983, **13**, 303.
13 O. Kahn, S. Sikorav, J. Gouteron, S. Jeannin, and Y. Jeannin, *Inorg. Chem.*, 1983, **22**, 2877.
14 S. Sikorav, I. Bkouche-Waksman, and O. Kahn, *Inorg. Chem.*, 1984, **23**, 490.
15 Y. Nakao, M. Yamazaki, S. Suzuki, W. Mori, A. Nakahara, K. Matsumoto, and S. Ooi, *Inorg. Chim. Acta*, 1983, **74**, 159.
16 J. Hornstra and B. Stubbe, PW1100 Data Processing Programs, Philips Research Laboratories, Eindhoven, Holland.
17 G. Germain, P. Main, and M. M. Woolfson, *Acta Crystallogr., Sect. B*, 1970, **24**, 274.
18 'International Tables for *X*-Ray Crystallography,' Kynoch Press, Birmingham 1974, vol. 4, pp. 71, 148.
19 C. K. Johnson, ORTEP, Report ORNL-3794, Oak Ridge National Laboratory, Oak Ridge, Tennessee, 1965.
20 'The Universal Crystallographic Computation Program System,' The Crystallographic Society of Japan, 1969.
21 I. M. Procter, B. J. Hathaway, and P. Nicholls, *J. Chem. Soc. A*, 1968, 1678.

22 W. E. Hatfield, in 'Theory and Applications of Molecular Paramagnetism,' eds. E. A. Boudreaux and L. N. Mulay, John Wiley, New York, 1976, p. 349.
23 G. L. Woolery, L. Powers, M. Winkler, E. I. Solomon, and T. G. Spiro, *J. Am. Chem. Soc.*, 1984, **106**, 86.
24 D. E. Wilcox, J. R. Long, and E. I. Solomon, *J. Am. Chem. Soc.*, 1984, **106**, 2186.

Received 12*th November* 1984; *Paper* 4/1923